

Calculation of the Electron Wave Function and Crystal Potential in a Sphalerite Semiconductor at a Given Temperature

O.P. Malyk

Lviv Polytechnic National University, 12, S. Bandera St., 79013 Lviv, Ukraine

(Received 22 August 2022; revised manuscript received 20 October 2022; published online 28 October 2022)

The article deals with a method of determining the energy spectrum, the electron wave function and the crystal potential in CdTe at an arbitrary given temperature. Using this approach, the temperature dependences of the ionization energies of intrinsic defects in cadmium telluride are calculated within the framework of the supercell method. The proposed method also makes it possible to define the temperature dependences of the optical and acoustic deformation potentials, as well as the temperature dependence of the parameters of electron scattering on ionized impurities, polar optical, piezooptical and piezoacoustic phonons. Within the framework of short-range scattering models, the temperature dependences of the electron mobility and Hall factor are considered.

Keywords: CdTe, Electron transport, Point defects, Ab initio calculation.

DOI: [10.21272/jnep.14\(5\).05007](https://doi.org/10.21272/jnep.14(5).05007)

PACS number: 72.20.Dp

1. INTRODUCTION

Usually, ab initio calculations of the energy characteristics of semiconductors make it possible to obtain the energy spectrum, wave function, and potential energy of an electron in a crystal. The obtained properties are assumed to describe the ground state of the crystal ($T=0$). In the current work, the author proposes a scheme for determining the above characteristics of a sphalerite semiconductor for an arbitrary predetermined temperature. The same characteristics of the semiconductor allow determining, at a given temperature, the parameters of electron scattering by defects of the crystal lattice, which in turn makes it possible to calculate the kinetic properties of the crystal at the same temperature.

The proposed method will be tested on the example of *n*-type cadmium telluride. This material plays an important role in the production of high-efficiency, low-cost, and thin-film solar cells. Therefore, the study of point defects in CdTe attracts widespread attention of researchers [1-7]. On the other hand, there are attempts in the literature to describe the transport phenomena in semiconductors, in particular in CdTe [8], which are based on DFT calculations [9-13]. However, a common shortcoming of these works is the lack of connection between the structure of point defects and the kinetic properties of CdTe, which determine the electronic properties of the material. In this paper, this problem will be solved, namely, the temperature dependence of the energy characteristics of the semiconductor and its point defects will be established, which will allow the temperature dependence of the kinetic properties of the semiconductor to be determined.

2. CALCULATION OF THE TEMPERATURE DEPENDENCES OF THE ELECTRON WAVE FUNCTION AND CRYSTAL POTENTIAL OF A SPHALERITE SEMICONDUCTOR

The description of transport phenomena in *n*-CdTe is based on the models of short-range electron scattering [8, 14-16]. The scattering models mentioned above

require the calculation of certain scattering constants, which in turn require the determination of the conduction band wave function and the crystal potential. Using preselected GGA exchange-correlation potentials for Cd and Te (pseudopotentials) and choosing a certain mixture of these conventional GGA exchange correlation potentials and the Hartree Fock exchange potential (this mixture is determined by the "exchmix" parameter of the ABINIT code), one can obtain the totality of mathematical solutions of the Schrödinger equation corresponding to the value of the parameter "exchmix" in the limits from 0 to 1. It should be noted that certain values of the "ecut" and "pawecutdg" parameters of the ABINIT code were used for the accuracy and convergence of the calculations. The parameter "ecut" has an enormous effect on the quality of the calculation; basically, the larger the "ecut", the better the calculation converges. The parameter "pawecutdg" defines the energy cut-off for the fine FFT grid, "pawecutdg" must be larger or equal to "ecut". The following values of these parameters were chosen in our calculations: "ecut" = 48 Ha, "pawecutdg" = 64 Ha. It should be noted that a further increase in these parameters leads to a change in the theoretical position of the energy levels of the electronic spectrum by approximately 1.2×10^{-5} eV, which is far beyond the accuracy of the experiment.

Using the calculation method described above, the physical solutions of the Schrödinger equation were separated from the totality of mathematical solutions of the Schrödinger equation for a sphalerite semiconductor (two different atoms in the unit cell). The criterion for selecting the physical solutions of the Schrödinger equation was chosen as follows: at a given temperature, the theoretical width of the band gap must coincide with its experimental value, which was determined from the experimental expression [17] for $\text{Hg}_{1-x}\text{Cd}_x\text{Te}$ solid solution:

$$E_g(x, T) = -0.302 + 1.93x - 0.81x^2 + 0.832x^3 + 5.35 \times 10^{-4} T(1 - 2x). \quad (1)$$

For sphalerite CdTe, this calculation was performed

by adjusting the theoretical band gap corresponding to $T = 0$ K (exchmix = 0.397) and $T = 300$ K (exchmix = 0.288). Herewith, the wave function of the electron in the conduction band and the potential energy of the electron in the crystal lattice at temperatures of 0 and 300 K were obtained. Based on these wave functions and crystal potentials, as well as using short-range scattering models [8, 14, 15], the following scattering constants can be calculated at 0 and 300 K, namely:

1) Electron-polar optical (PO) phonon, electron-piezoacoustic (PAC) phonon and electron-piezo-optic (POP) phonon scattering constants [8, 14, 15]:

$$A_{PO} = A_{PAC} = A_{POP} = \int \psi^* (R^2 - r^2 / 3) \psi \, dr. \quad (2)$$

The region of integration includes two atoms of different sorts, its volume is equal to 1/8 of the volume of the sphalerite elementary cell, ψ stands for the electron wave function in the sphalerite elementary cell.

2) d_0 is the optical deformation potential constant which was chosen as a maximum value among three optical deformation potential constants corresponding to one longitudinal and two transverse branches of the lattice optical vibrations:

$$d_{0\nu} = a_0 \int \psi^* \varepsilon_\nu \cdot \mathbf{V} \psi \, dr, \quad \nu=1,2,3, \quad (3)$$

where the region of integration is the same as in the case of PO scattering; ε_ν denotes the unitary contravariant polarization vector of the optical oscillations and the vector \mathbf{V} is expressed in terms of the derivatives of the self-consistent electron potential energy over the coordinates of the atoms of the unit cell [15].

3) E_{AC} is the acoustic deformation potential constant which was chosen as a maximum value among three acoustic deformation potential constants corresponding to one longitudinal and two transverse branches of the lattice acoustic vibrations [8]:

$$\begin{aligned} E_{AC||} &= -(I_1/4 + I_2/2 + I_3/2), \\ E_{AC\perp 1} &= -(I_1/4 - I_2/4 + I_3/2), \\ E_{AC\perp 2} &= -(I_1/2 + I_2/2 - I_3/4), \end{aligned} \quad (4)$$

where

$$I_1 = \int \psi^* V_1 \psi \, dr'; I_2 = \int \psi^* V_2 \psi \, dr'; I_3 = \int \psi^* V_3 \psi \, dr'; V_1; V_2; V_3'$$

are the components of the vector \mathbf{V} in the oblique coordinate system created by the primitive vectors of the zinc blende structure and the region of integration is the same as in the case of PO scattering.

4) The ionized impurity scattering constant

$$A_{II} = \int_{\Omega} \Psi^* \frac{1}{r} \Psi \, dr, \quad (5)$$

where integration is carried out throughout the sphalerite elementary cell.

As it is seen from (2)-(5), the scattering constants of the short-range models are represented as integrals over the wave function Ψ and the crystal potential U . These integrals were evaluated using three-dimensional B -spline interpolation and the finite displacement method [8]. Since Ψ and U depend on temperature, the scat-

tering constants also depend on temperature. Assuming a linear temperature dependence, one can obtain the dependence of the scattering parameters on temperature:

$$A_{PO} = (12.24 + 2.088 \times 10^{-4} T) \times 10^{-20} m^2, \quad (6a)$$

$$d_0 = -20.93 - 4.053 \times 10^{-3} T \text{ eV}, \quad (6b)$$

$$E_{AC} = -2.423 - 4.628 \times 10^{-4} T \text{ eV}, \quad (6c)$$

$$A_{II} = (0.4794 - 7.405 \times 10^{-6} T) \times 10^{10} m^{-1}. \quad (6d)$$

Using these relations, one can calculate the temperature dependences of electron transition probabilities and the kinetic coefficients of cadmium telluride.

3. DETERMINATION OF THE TEMPERATURE DEPENDENCES OF THE DONOR IONIZATION ENERGY OF DIFFERENT TYPES OF DEFECTS

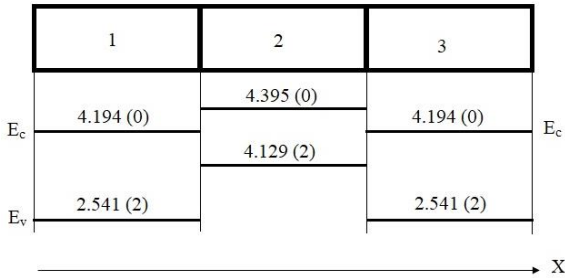
The proposed study considers the intrinsic donor defects, namely, Cd_{Te}, Te_{Cd}, V_{Te}, Te_{Cd} - Cd_{Te}, V_{Te} - Cd_{Te}. The energy spectrum of the defect structure was calculated using the supercell method (1×1×2 sphalerite cubic structure) based on the ABINIT code: for Cd_{Te} - supercell Cd₉Te₇; Te_{Cd} - supercell Cd₇Te₉; V_{Te} - supercell Cd₈Te₇; Te_{Cd} - Cd_{Te} - supercell Cd₈Te₈; V_{Te} - Cd_{Te} - supercell Cd₉Te₆. In addition, the energy spectrum of the ideal Cd₈Te₈ supercell was calculated. To calculate the energy spectrum of ideal and defective supercells, it is necessary to have pseudopotentials of Cd and Te atoms. The pseudopotentials for Cd and Te atoms were obtained by means of the AtomPAW (atompaw v3.0.1.9 and AtomPAW2Abinit v3.3.1) code. The PAW functions were generated for the following valence basis states: 5s²5p⁰4d¹⁰ for Cd and 4s²5s²4p²5p⁴ for Te. The radii of the augmentation spheres r_{PAW} have the following values: 2.2 and 2.4 for Cd and Te, respectively. The exchange and correlation effects were taken into account within the density functional theory (DFT), namely in generalized gradient approximation (GGA) formalism suggested by Perdew, Burke and Ernzerhof (PBE) [18]. The output files of the AtomPAW code contain the full set of data which are input parameters for initiation of the ABINIT code. The results of calculations of energy spectrums of these supercells are presented in Table 1.

The idea of applying the method of supercells is as follows. Let the X axis be directed along the rib of an ideal (defective) supercell with length a_0 (Fig. 1). Then the Y axis is directed along the rib of the supercell with length a_0 , and the Z axis is directed along the rib of the supercell with length $2a_0$. In the nodes of the ideal (defective) supercell, located on the border of the supercell, there are Cd atoms, and Te atoms are inside the ideal (defective) supercell. The crystal defect is always located inside the defective supercell. Next, for the point Γ , the energy spectrum for the ideal and defective supercells is calculated using the corresponding value of the parameter exchmix of ABINIT code (see Table 1). It should be noted that the coordinate system used in each individual supercell is not related to the coordinate system in the other supercell. The proposed method is very similar to the method used in Riemann geometry, namely a three-dimensional manifold (in our

Table 1 – Energy spectrum of ideal and defect supercells (1×1×2 sphalerite cubic structure)

$T = 0, E_g = 1.65 \text{ eV}, \text{exchmix} = 0.09$			$T = 300 \text{ K}, E_g = 1.48 \text{ eV}, \text{exchmix} = 0.0182$		
Energy levels of ideal Cd ₈ Te ₈ , eV	Energy levels of defects, eV	Ionization energy, eV	Energy levels of ideal Cd ₈ Te ₈ , eV	Energy levels of defects, eV	Ionization energy, eV
$E_c = 1 \times (4.194) (0)$ $E_v = 2 \times (2.541) (2)^*$	Cd _{Te} 2×(4.395) (0) 1×(4.129) (2) 1×(2.453) (2)	$\Delta E_D = 0.065$	$E_c = 1 \times (4.108) (0)$ $E_v = 2 \times (2.620) (2)$	Cd _{Te} 2×(4.395) (0) 1×(4.132) (2) 1×(2.495) (2)	$\Delta E_D = -0.024$
$E_c = 1 \times (4.194) (0)$ $E_v = 2 \times (2.541) (2)$	Tec _d 1×(4.149) (0) 2×(3.792) (0) 1×(3.402) (2)	$\Delta E_D = 0.792$	$E_c = 1 \times (4.108) (0)$ $E_v = 2 \times (2.620) (2)$	Tec _d 1×(4.096) (0) 2×(3.805) (0) 1×(3.410) (2)	$\Delta E_D = 0.698$
$E_c = 1 \times (4.194) (0)$ $E_v = 2 \times (2.541) (2)$	V _{Te} 1×(4.233) (0) 1×(2.461) (2)	neutral defect	$E_c = 1 \times (4.108) (0)$ $E_v = 2 \times (2.620) (2)$	V _{Te} 1×(4.200) (0) 1×(2.435) (2)	neutral defect
$E_c = 1 \times (4.194) (0)$ $E_v = 2 \times (2.541) (2)$	Tec _d – Cd _{Te} 1×(4.094) (0) 1×(3.886) (0) 1×(3.801) (2)	$\Delta E_D = 0.393$	$E_c = 1 \times (4.108) (0)$ $E_v = 2 \times (2.620) (2)$	Tec _d – Cd _{Te} 1×(4.090) (0) 1×(3.886) (0) 1×(3.795) (2)	$\Delta E_D = 0.313$
$E_c = 1 \times (4.194) (0)$ $E_v = 2 \times (2.541) (2)$	V _{Te} – Cd _{Te} 1×(3.863) (0) 1×(3.487) (0) 1×(3.419) (2)	$\Delta E_D = 0.775$	$E_c = 1 \times (4.108) (0)$ $E_v = 2 \times (2.620) (2)$	V _{Te} – Cd _{Te} 1×(3.856) (0) 1×(3.474) (0) 1×(3.373) (2)	$\Delta E_D = 0.735$

*Notation 2×(2.541) (2) means that there exists a 2-fold degenerate energy level with an occupation number equal to 2


Fig. 1 – Location along the X axis of ideal and defective supercells and the corresponding positions of the energy levels for ideal supercells and Cd_{Te} defect at $T = 0 \text{ K}$. 1, 3 – ideal Cd₈Te₈ supercell, 2 – defective Cd₈Te₇ supercell

case a crystal) is described by a set of individual coordinate systems used in a certain region of manifold (in our case a supercell). So, in this case, a crystal is a set of ideal supercells (for which the theoretical value of the band gap coincides with the experiment) and a certain number of defective supercells.

As an example, the calculation of ionization energy of the defect will be used for the Cd_{Te} defect. Comparing at $T = 0 \text{ K}$ the energy levels of the ideal Cd₈Te₈ structure with the energy levels of the defect, the transition of the electron from the defect level 1×(4.129) (2) to the conduction band level of the ideal structure 1×(4.194) (0) (with ionization energy $\Delta E_D = 0.065 \text{ eV}$) is seen to be most probable (Fig. 1 and Table 1). The remaining electronic transitions are unlikely due to very high ionization energy. At $T = 300 \text{ K}$, the electrons from the defect level 1×(4.132) (2) will pass to the level of the conduction band 1×(4.108) (0), i.e., there occurs a complete ionization of the defect (ionization energy is negative and equal to $\Delta E_D = -0.024 \text{ eV}$). Other electron transitions are unlikely due to high ionization energy. Assum-

ing a linear temperature dependence of the defect ionization energy, this dependence can be determined. Similarly, the temperature dependences of the ionization energy of other types of defects can be analyzed. Analytical expressions for these dependences have the form:

$$\text{CdTe: } \Delta E_D = 0.065 - 2.967 \times 10^{-4} T, \quad (7a)$$

$$\text{Tecd: } \Delta E_D = 0.792 - 3.133 \times 10^{-4} T, \quad (7b)$$

$$\text{Tecd} - \text{CdTe: } \Delta E_D = 0.393 - 2.667 \times 10^{-4} T, \quad (7c)$$

$$\text{VTe} - \text{CdTe: } \Delta E_D = 0.775 - 1.333 \times 10^{-4} T. \quad (7d)$$

It should be noted that for Cd_{Te} the level of the discrete defect merges with the conduction band at $T = 219 \text{ K}$. For other types of defects, with the temperature increasing, there is only a decrease in ionization energy without merging with the conduction band.

4. DISCUSSION

Theoretical calculations were compared with experimental data for undoped cadmium telluride [19]. Only defects with the lowest ionization energy were taken into account in the calculations, as they make the dominant contribution to the transport phenomena. As can be seen from (7a), for undoped cadmium telluride such a defect is Cd_{Te}. Given the merger of this defect level with the conduction band, an electroneutrality equation for the Fermi level can be written in the form:

$$1) \quad n - p = N_D \sqrt{1 + 2 \exp\left(\frac{F - E_D}{k_B T}\right)} \quad \text{at } T < 219 \text{ K};$$

$$2) \quad n - p = N_D \quad \text{at } T > 219 \text{ K}.$$

The temperature dependences of the electron mobility were calculated on the basis of short-range scattering models [8, 14, 15] within the framework of the exact solution of the Boltzmann kinetic equation [20].

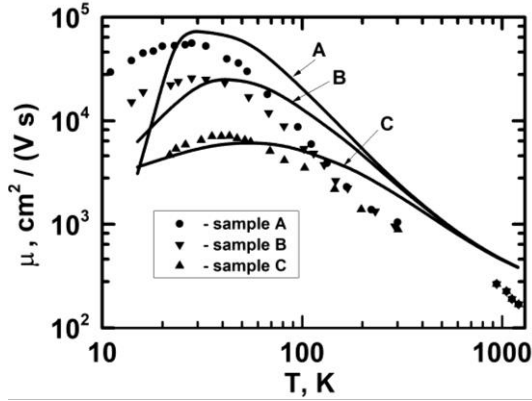


Fig. 2 – Temperature dependences of electron mobility in undoped *n*-CdTe. Experimental data – [23]

For undoped samples, the following defect concentration values were obtained: sample A – $N_D=5 \times 10^{14} \text{ cm}^{-3}$, $N_{SS}=8 \times 10^{14} \text{ cm}^{-3}$ (concentration of the static strain (SS) centres); sample B – $N_D=5 \times 10^{15} \text{ cm}^{-3}$, $N_{SS}=2.5 \times 10^{15} \text{ cm}^{-3}$; sample C – $N_D=5 \times 10^{16} \text{ cm}^{-3}$, $N_{SS}=1.1 \times 10^{16} \text{ cm}^{-3}$. The defect concentration values give a sufficiently good coinciding with experimental temperature dependences of electron mobility (see Fig. 2). However, at low temperatures and low defect concentrations, some deviation of the theoretical curves from the experimental data is observed. This can be explained by the insufficiently successful choice of the initial pseudopotentials of cadmium and tellurium.

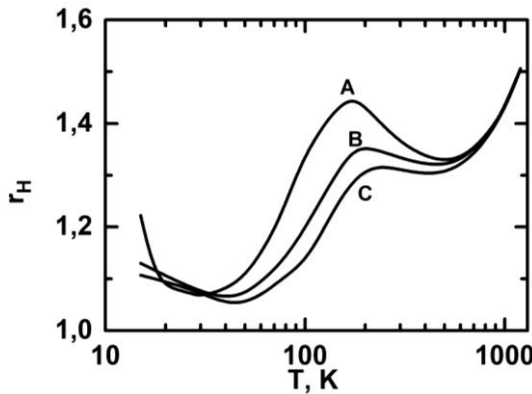


Fig. 3 – Temperature dependence of the electron Hall factor in undoped *n*-CdTe. The notations of the curves correspond to the crystals in Fig. 2

The abovementioned method of calculation allows the temperature dependence of the electron’s Hall factor for undoped samples to be obtained (Fig. 4). These dependences have minima corresponding to the temperature at which the transition from the SS-scattering mechanism to the PO-scattering mechanism occurs. From Fig. 3, it is seen that the higher the concentration of defects, the higher the transition temperature.

If we compare the theoretical curves obtained by the above method with the theoretical curves obtained in the relaxation time approximation (Fig. 4 for undoped samples), one can see that the relaxation time approximation gives theoretical curves that are much less consistent with experiment (curve 1 corresponds to the low-temperature region $\hbar\omega \gg k_B T$ and curve 2 cor-

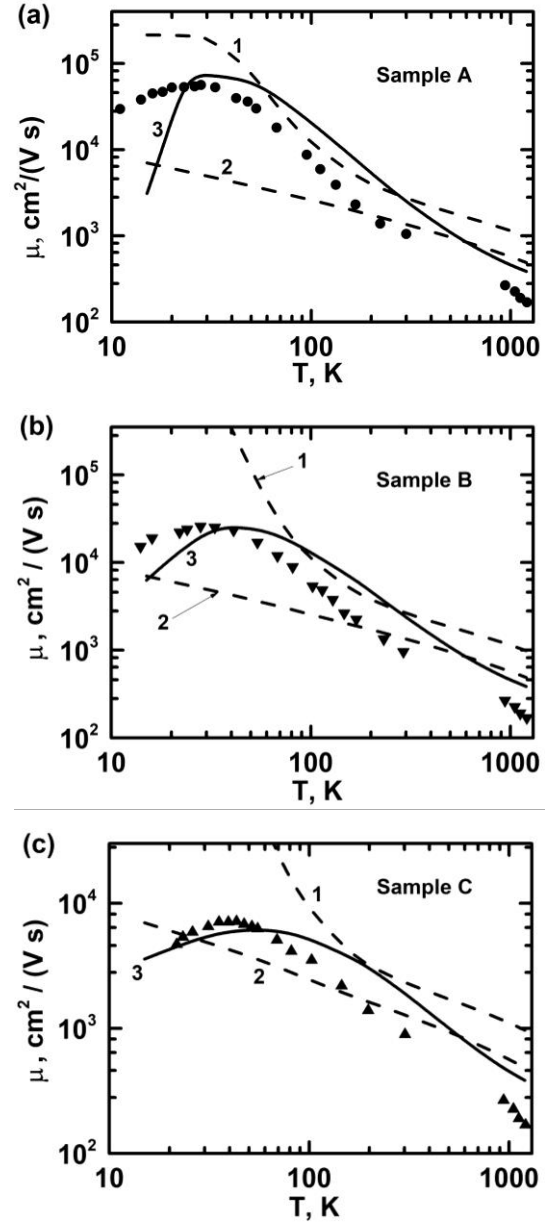


Fig. 4 – Comparison of the theoretical curves obtained in the framework of long-range (curves 1 and 2) and short-range (curve 3) scattering models for undoped samples. Here, (a) sample A: $N_D = 5 \times 10^{14} \text{ cm}^{-3}$; $N_{SS} = 8 \times 10^{14} \text{ cm}^{-3}$; (b) sample B: $N_D = 5 \times 10^{15} \text{ cm}^{-3}$; $N_{SS} = 2.5 \times 10^{15} \text{ cm}^{-3}$; and (c) sample C: $N_D = 5 \times 10^{16} \text{ cm}^{-3}$; $N_{SS} = 1.1 \times 10^{16} \text{ cm}^{-3}$

responds to the high-temperature region $\hbar\omega \ll k_B T$ in the relaxation time approximation) especially in the region of high defect concentrations. For CdTe, the Debye temperature is $\theta_D = 239 \text{ K}$. This means that the low-temperature region will be determined by the condition $T < 24 \text{ K}$, and the high-temperature region will be determined by the condition $T > 2400 \text{ K}$. Therefore, $24 \text{ K} \ll T \ll 2400 \text{ K}$ temperature region corresponds to inelastic scattering, where the relaxation time approximation is not valid. On the other hand, the short-range scattering models allow to describe inelastic scattering. This indicates that the method proposed in this article more adequately describes the defect structure of crystals and their kinetic properties.

5. CONCLUSIONS

The author proposes a new scheme for calculating the energy spectrum, wave function and potential energy of an electron in a crystal at a given temperature. Based on this, the temperature dependences of defect

parameters and kinetic coefficients are calculated. It should be noted that the proposed calculation method can be applied to all semiconductors with a sphalerite structure. The difference between the calculations carried out in the work will be the use of other pseudopotentials of atoms of the basic substance and impurities.

REFERENCES

1. I. Sankin, D. Krasikov, *phys. status solidi a* **215**, 1800887 (2019).
2. Su-Huai Wei, S.B. Zhang, *Phys. Rev. B: Condens. Matter Mater. Phys.* **66**, 155211 (2002).
3. Jie Ma, Su-Huai Wei, T.A. Gessert, Ken K. Chin, *Phys. Rev. B: Condens. Matter Mater. Phys.* **83**, 245207 (2011).
4. Ji-Hui Yang, Wan-Jian Yin, Ji.-Sang. Park, Jie Ma, Su-Huai Wei, *Semicond. Sci. Technol.* **31**, 083002 (2016).
5. D. Krasikov, A. Knizhnik, B. Potapkin, S. Selezneva, T. Sommerer, *Thin Solid Films* **535**, 322 (2013).
6. W. Orellana, E. Menendez-Proupin, M. A. Flores, *phys. status solidi b* **256**, 1800219 (2019).
7. I. Sankin, D. Krasikov, *J. Mater. Chem. A* **5**, 3503 (2017).
8. O. Malyk, S. Syrotyuk, *Comput. Mater. Sci.* **139**, 387 (2017).
9. K. Kaasbjerg, K.S. Thygesen, K.W. Jacobsen, *Phys. Rev. B* **85**, 115317 (2012).
10. O. Restrepo, K. Varga, S. Pantelides, *Appl. Phys. Lett.* **94**, 212103 (2009).
11. O.D. Restrepo, K.E. Krymowski, J. Goldberger, W.A. Windl, *New J. Phys.* **16**, 105009 (2014).
12. X. Li, J.T. Mullen, Z. Jin, K.M. Borysenko, M. Buongiorno Nardelli, K.W. Kim, *Phys. Rev. B* **87**, 115418 (2013).
13. Wu. Li, *Phys. Rev. B* **92**, 075405 (2015).
14. O.P. Malyk, S.V. Syrotyuk, *J. Electron. Mater.* **47**, 4212 (2018).
15. O.P. Malyk, *J. Electron. Mater.* **49**, 3080 (2020).
16. O.P. Malyk, *Can. J. Phys.* **92**, 1372 (2014).
17. G.L. Hansen, J.L. Schmit, T.N. Casselman, *J. Appl. Phys.* **53**, 7099 (1982).
18. J. P. Perdew, K. Burke, M. Ernzerhof, *Phys. Rev. Lett.* **77**, 3865 (1996).
19. B. Segall, M.R. Lorenz, R.E. Halsted, *Phys. Rev.* **129**, 2471 (1963).
20. O.P. Malyk, *J. Alloy. Compd.* **371** No 1-2, 146 (2004).

Розрахунок електронної хвильової функції та потенціалу кристала в напівпровіднику зі структурою сфалериту при заданій температурі

О.П. Малик

Національний університет «Львівська політехніка, вул. С. Бандери, 12, 29013 Львів, Україна

У статті розглянуто метод визначення енергетичного спектру, хвильової функції електрона та кристалічного потенціалу в CdTe при довільно заданій температурі. За допомогою цього підходу в рамках методу суперкомірки розраховано температурні залежності енергій іонізації власних дефектів в телурид кадмію. Запропонований метод також дає змогу визначити температурні залежності оптичного та акустичного потенціалів деформації, а також температурну залежність параметрів розсіювання електронів на іонізованих домішках, полярних оптичних, п'єзооптичних та п'єзоакустичних фононах. У рамках близькодючих моделей розсіяння розглядаються температурні залежності рухливості електронів і фактора Холла.

Ключові слова: CdTe, Перенесення електронів, Точкові дефекти, Ab initio розрахунок.